

Ash admixtures formed during the loss on ignition (LOI) procedure and their impact on laser textural analysis results [supplementary material]

Dmitry Tsvirko¹, Wojciech Tołoczko², Piotr Kittel³

¹ University of Lodz, Doctoral School of Exact and Natural Sciences, Łódź, Poland,

e-mail: dzmitry.tsvirka@edu.uni.lodz.pl (corresponding author), ORCID ID: 0000-0002-5913-050X

² University of Lodz, Faculty of Geographical Sciences, Department of Physical Geography, Łódź, Poland,

e-mail: wojciech.toloczko@geo.uni.lodz.pl, ORCID ID: 0000-0001-5441-4418

³ University of Lodz, Faculty of Geographical Sciences, Department of Geology and Geomorphology, Łódź, Poland,

e-mail: piotr.kittel@geo.uni.lodz.pl, ORCID ID: 0000-0001-6987-7968

Table S1

The decrease in the mass of the studied samples after 8-hour ignition in a muffle furnace at 550°C

Sample number	Sample depth [cm]	Mass of the entire sample before ignition (M), dried at 105°C [g]	Ash mass immediately after the muffle furnace (M_{8h}) [g]	LOI ₅₅₀ [%]	Lithological unit
3	10–15	5.318	2.609	50.94	Brown telmatic peat
4	15–20	7.066	4.134	41.49	
5	20–23	6.055	3.880	35.92	
6	23–28	3.845	2.641	31.31	
7	28–33	12.140	9.328	23.16	Black telmatic peat
8	33–35	11.278	9.610	14.79	
9	35–40	10.132	7.113	29.80	
10	40–45	10.086	4.265	57.71	
11	45–49	8.840	1.495	83.09	Coarse detritus gyttja
12	49–55	9.162	1.579	82.77	
13	55–60	7.700	1.441	81.29	
14	60–65	6.081	0.998	83.59	
15	65–70	4.984	0.767	84.61	
31	142–146	12.303	11.570	5.96	Fine-medium sand
32	146–150	14.965	14.409	3.72	

Explanation: LOI₅₅₀ – loss on ignition at 550°C.

Table S2

An additional experiment conducted on highly organic samples taken from the core PKK-1-2

Sample number	Sample depth [cm]	LOI ₅₅₀ [%]	Ash mass immediately after the muffle furnace [mg]	Masses at room temperature		Mass loss [%]	Remarks
				Dry ash before HCl treatment [mg]	Dry ash after HCl treatment [mg]		
16	70–75	85.230	266	380	120	68.42	Coarse detritus gytija. Strong CO ₂ emission visible during the reaction of ash with HCl
17	75–80	87.879	168	320	60	81.25	
18	80–85	86.993	218	420	110	73.81	
19	85–90	76.417	362	660	420	36.36	
20	90–95	74.274	425	900	600	33.33	
21	95–100	75.583	461	910	600	34.07	
22	100–105	72.921	368	1020	690	32.35	
23	105–110	69.327	615	1250	920	26.40	
24	110–115	75.247	476	1100	780	29.09	
28	130–135	70.876	685	1680	1270	24.40	

Explanations: The table displays the mass loss of the ash following APP. Values in bold are highly organic samples that experienced only a minor ash mass loss after APP.

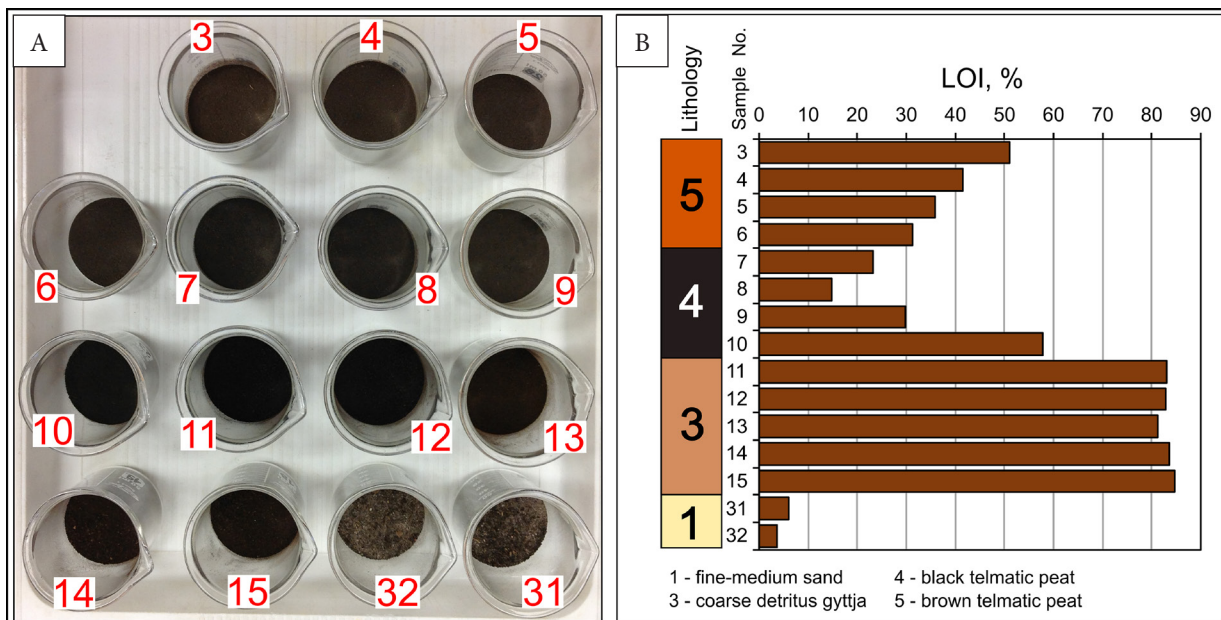


Fig. S1. Studied fifteen samples from the core PKK-1-2: A) samples containing organic matter before ignition in a muffle furnace, with their numbers (photo by D. Tsvirko, 2022); B) the initial loss on ignition results with lithological column

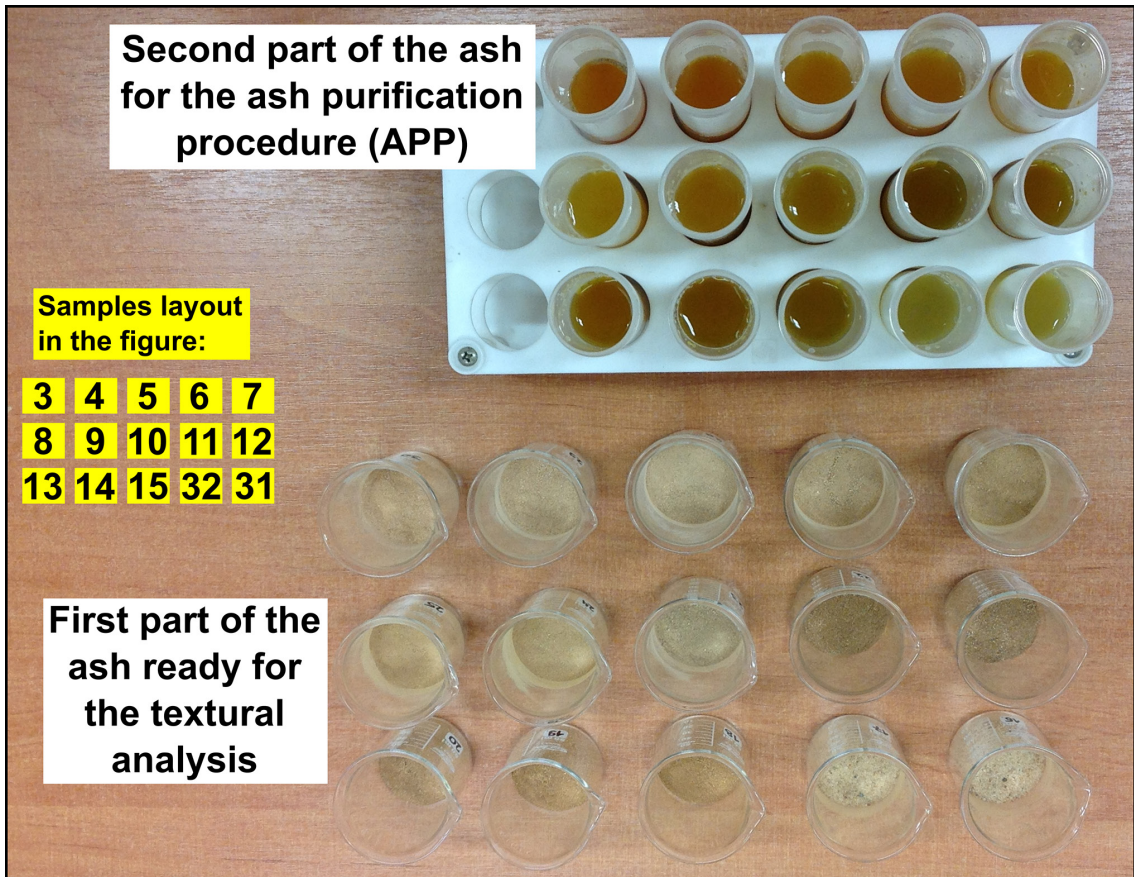


Fig. S2. Studied ash samples divided into two parts, part of the ash was mixed with 10% HCl in test tubes (photo by D. Tsvirko, 2022)



Fig. S3. Test tubes with a mixture of ash and HCl acid in a water bath (photo by D. Tsvirko, 2022)

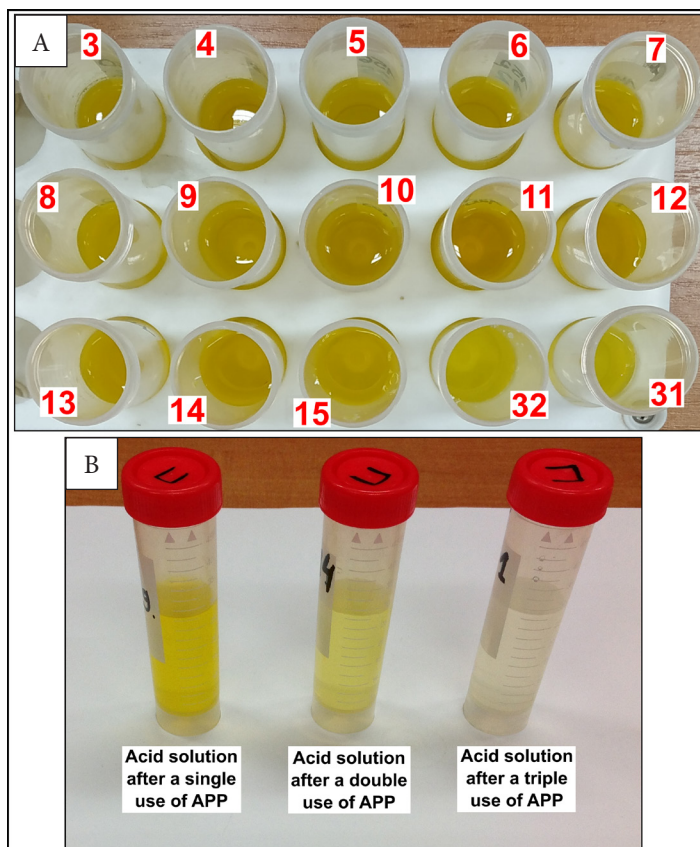


Fig. S4. Centrifuged yellowish HCl solutions after undergoing APP, along with their corresponding numbers (photos by D. Tsvirko, 2022): A) solutions that underwent a single APP treatment; B) solutions from sample 14 after a single, double, and triple APP treatment



Fig. S5. Spectrophotometer SPEKOL11 (photo by D. Tsvirko, 2022)

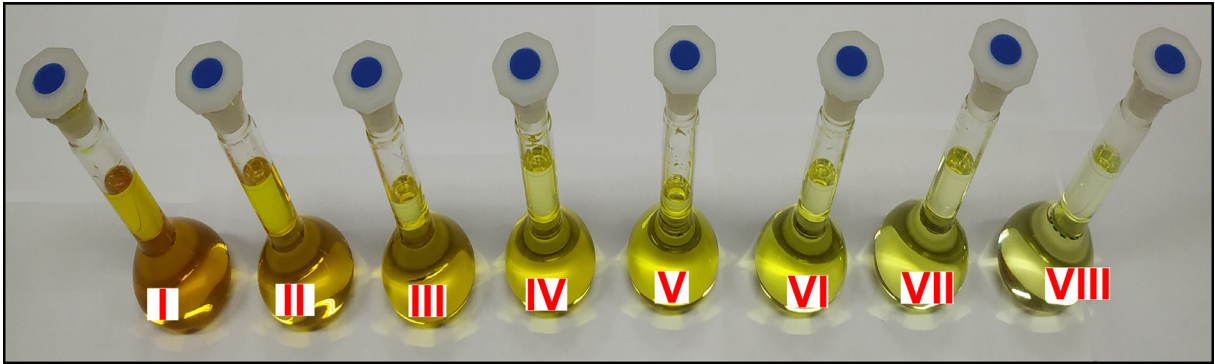


Fig. S6. Reference 10% HCl solutions with a known mass and concentration of iron. These solutions were prepared from FeCl_3 powder and each solution has a volume of 50 mL (photo by D. Tsvirko, 2022)

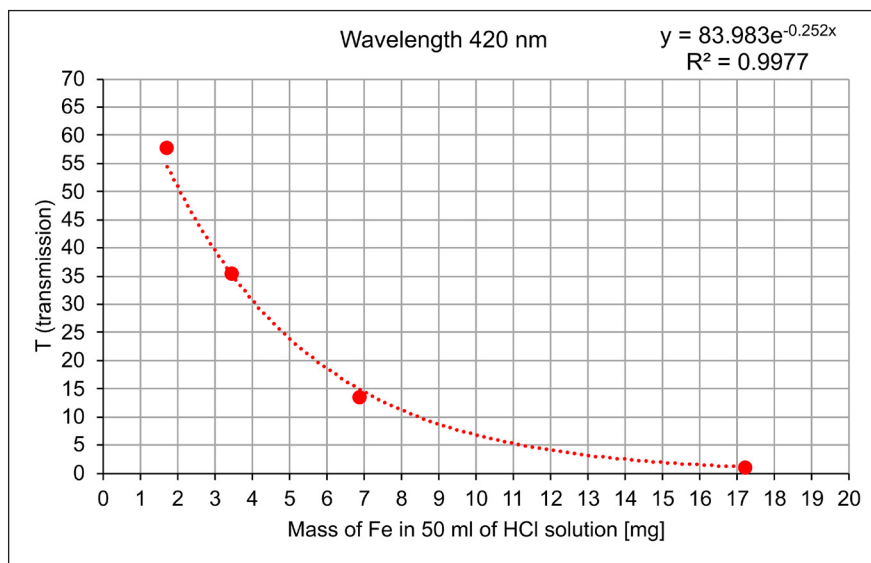


Fig. S7. Relationship between the transmission (T) and content of iron (Fe) in milligrams, in 50 mL of 10% HCl solution at a wavelength of 420 nm, with an exponential trend line

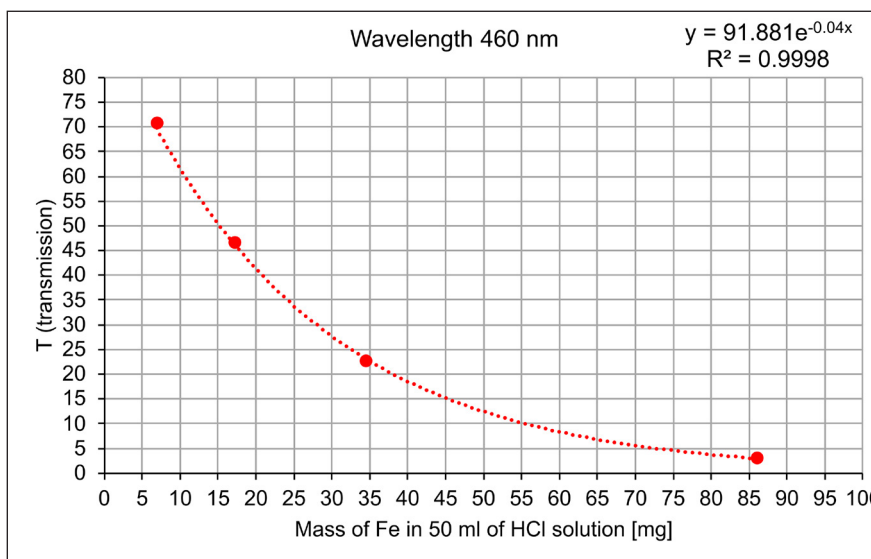


Fig. S8. Relationship for a wavelength of 460 nm (see description of Figure S7)

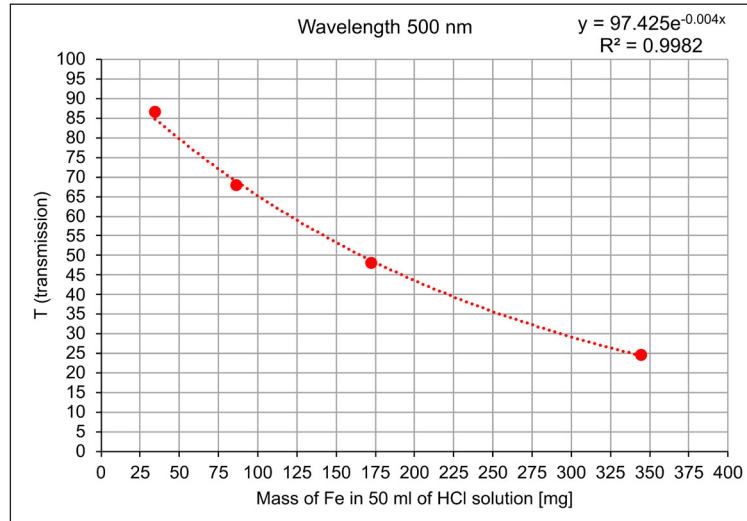


Fig. S9. Relationship for a wavelength of 500 nm (see description of Figure S7)



Fig. S10. Malvern Panalytical Mastersizer 3000 for laser textural (particle size distribution) analysis (photo by D. Tsvirko, 2022)

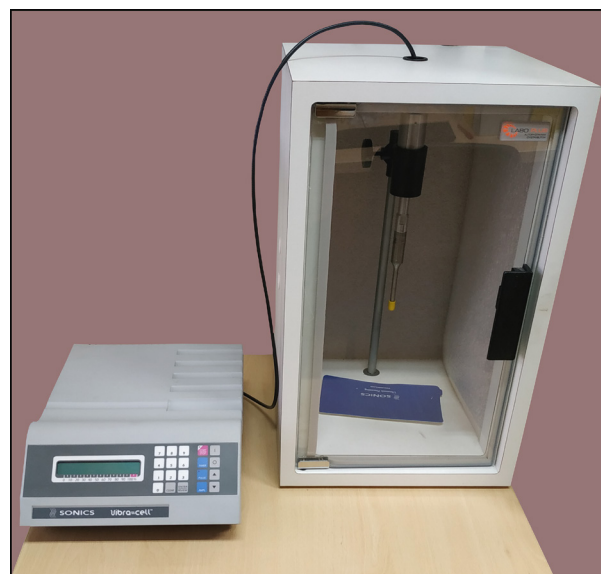


Fig. S11. Ultrasonic Processor Sonicator VCX 130 for particle disaggregation (photo by D. Tsvirko, 2022)